Discontinuous Hermite Collocation and IMEX Runge-Kutta for a Treated Quasi-linear Heterogeneous Brain Tumor Model

I. E. Athanasakis[‡], E. P. Papadopoulou[†] and Y. G. Saridakis[‡]

Abstract—Over the past few years several mathematical models have been developed to simulate and study the growth of treated or untreated aggressive forms of brain tumors. Encouraged by our recent results on the development of fourth order Discontinuous Hermite Collocation (DHC) numerical schemes to approximate the classical solution of parabolic evolution problems, in the present work we consider employing the DHC method for the solution of a quasi-linear tumor growth model which, apart from proliferation and diffusion, incorporates as well the effects from radiotherapy and chemotherapy. The model is also being characterized by a discontinuous diffusion coefficient to incorporate the heterogeneity of the brain tissue. To study the spatiotemporal dynamics of the model problem, the DHC spatial discretization is coupled with Implicit-Explicit (IMEX) Runge-Kutta (RK) third order schemes for the time discretization. The effectiveness of the resulting DHC-RK method is being demonstrated through several numerical experiments.

Keywords—High-grade Gliomas, Radiotherapy, Chemotherapy, Reaction-Diffusion PDEs, Discontinuous Hermite Collocation, Implicit-Explicit Runge-Kutta.

I. Introduction

HIGH-GRADE GLIOMAS are among the most common and aggressive forms of primary brain tumors. The most typical problem in diagnosis and treatment of patients with high-grade glioma, even after an extensive surgical procedure, is the rapid infiltration of tumor cells in adjacent normal tissue. Postoperative therapeutic treatment, such as radiotherapy and chemotherapy, is considered absolutely necessary to reduce tumor expansion.

As gliomas are known to consist of motile cells able to proliferate as well as migrate, well known and successful mathematical models, such as [11], [27], [28] and [9] (for a review see [13]), have been using reaction-diffusion evolution equations to describe the core spatiotemporal model's dynamics. The incorporation of brain's tissue heterogeneity (white-grey matter) was achieved in [19], [25] and [26] by introducing an appropriately discontinuous diffusion coefficient.

Recently, in [20], the effects of low-dose-rate radiotherapy, as a generalized linear quadratic model, and chemotherapy, as a simple log-kill model, were incorporated into a logistic growth reaction-diffusion model and several different schedules of sequential or combined therapy were studied in detail. A very interesting approach, as it pertains to radiotherapy modeling, was also presented in [10] (see also [21]) where a patient-specific, biologically optimized radiotherapy plan was presented.

Collocation (cf. [22], [8]) is an easily implemented spatial discretization method for BVPs that requires no numerical integration as it does not rely on a variational formulation. Combined with third degree finite element basis function, such as Hermite cubic or Spline elements, produces fourth order approximations to sufficiently smooth solutions.

Since the introduction of a class of discontinuous Hermite elements and their combined usage with the Collocation method (cf. [15], [16]), for the treatment of linear reaction-diffusion problems with discontinuous diffusion coefficients, the method has been also coupled (cf. [3], [4]) with high order Runge-Kutta to increase performance and stability.

Following our recent results in [3] and [4], the main objective in this work is to study the performance of the DHC method, combined with Implicit-Explicit Runge-Kutta schemes, as it pertains to the solution of the logistic quasi-linear heterogeneous brain tumor invasion model that also incorporates the effects from radiotherapy and chemotherapy. In the present study we include the results from the 1+1 dimension case, while the results for higher dimensions will be presented elsewhere (cf. [5]).

II. Methodology

A. The Mathematical Model

The core model PDE, that describes heterogeneous brain tumor invasion (cf. [19]) and incorporates the effects from radiotherapy and chemotherapy (cf. [20], [21]), is given in the form:

$$\frac{\partial \bar{c}}{\partial \bar{t}} = \nabla \cdot \left(\bar{D}(\bar{x})\nabla \bar{c}\right) + \rho \bar{c}(1 - \frac{\bar{c}}{c_k}) - \bar{R}(\bar{c},\bar{t}) - \bar{G}(\bar{c},\bar{t}) \ , \quad (1)$$

where $\bar{c}(\bar{x},\bar{t})$ denotes the tumor cell density, ρ denotes the net proliferation rate, c_k denotes the carrying capacity and $\bar{D}(\bar{\mathbf{x}})$ is the diffusion coefficient representing the active motility of malignant cells satisfying

$$\bar{D}(\bar{x}) = \begin{cases} D_g & , \ \bar{x} \in \bar{\Omega}_g \text{ Grey Matter} \\ D_w & , \ \bar{x} \in \bar{\Omega}_w \text{ White Matter} \end{cases} , \quad (2)$$

with D_g and D_w scalars and $D_w > D_g$, since glioma cells migrate faster in white than in grey matter.

Manuscript received May 31, 2015; revised June 30, 2015.

[‡]School of Production Engineering and Management, Applied Math & Computers Laboratory, Technical University of Crete, 73100 Chania, Greece

[†]School of Mineral Resources Engineering, Applied Math & Computers Laboratory, Technical University of Crete, 73100 Chania, Greece

Email of the corresponding author : y.saridakis@amcl.tuc.gr

The term $\bar{R}(\bar{c},\bar{t})$ denotes low-dose-rate and fractionated radiotherapy, and is defined by (cf. [14], [20] and the relevant references therein):

$$\bar{R}(\bar{c},\bar{t}) = \begin{cases} R_{\text{eff}} k_R(\bar{t})\bar{c} & , \quad \bar{t} \in \left(\bar{T}_{R_0}, \bar{T}_{R_1}\right] \text{ (therapy on)} \\ 0 & , \quad \bar{t} \notin \left(\bar{T}_{R_0}, \bar{T}_{R_1}\right] \text{ (therapy off)} \end{cases} \tag{3}$$

where $k_R(\bar{t})$ denotes the temporal profile of the radiation schedule and, by using a time step of one day, is simply one on therapy days and zero otherwise. R_{eff} denotes the effect of n fractions per day and is given by

$$R_{\text{eff}} = nd\left\{\alpha + 2\beta d\left[g(\mu\tau) + 2\left(\frac{\cosh(\mu\tau)-1}{(\mu\tau)^2}\right)h_n(\phi)\right]\right\} \tag{4}$$

with

$$g(\mu\tau) = \tfrac{\mu\tau-1+e^{-\mu\tau}}{(\mu\tau)^2} \quad \text{and} \quad h_n(\phi) = \tfrac{(n-1-n\phi+\phi^n)\phi}{n(1-\phi)^2}\ , \tag{5}$$

where α and β are sensitivity parameters, d is the dose rate, μ is the half time for repair of DNA damage, τ is the irradiation duration and $\phi = e^{-\mu(\tau+\Delta\tau)}$ with $\Delta\tau$ denoting the time interval between fractions.

In analogy to the radiotherapy equation in (3), the term $\bar{G}(\bar{c},\bar{t})$ denotes the effect of chemotherapy and, assuming a simple log-kill mode, is defined by (cf. [20] and the relevant references therein) :

$$\bar{G}(\bar{c},\bar{t}) = \begin{cases} k_G(\bar{t})\bar{c} & , \quad \bar{t} \in \left(\bar{T}_{G_0}, \bar{T}_{G_1}\right] \text{ (therapy on)} \\ 0 & , \quad \bar{t} \notin \left(\bar{T}_{G_0}, \bar{T}_{G_1}\right] \text{ (therapy off)} \end{cases} \tag{6}$$

and $k(\bar{t})$ is proportional to the drug concentration.

On the anatomy boundaries zero flux boundary conditions are imposed while for $\bar{t}=0$ an initial spatial distribution of malignant cells $\bar{c}(\bar{x},0) = \bar{f}(\bar{x})$ is assumed.

Using the dimensionless variables:

$$x = \sqrt{\frac{\rho}{D_w}}\bar{x} \ , \quad t = \rho\bar{t} \ , \quad c(x,t) = \frac{1}{c_k}\bar{c}\left(\sqrt{\frac{\rho}{D_w}}\bar{x},\ \rho\bar{t}\right) \ ,$$

$$D = \frac{\bar{D}}{D_w} \ , \ R = R(t) = \frac{R_{\text{eff}} k_R(\rho\bar{t})}{\rho} \ , \ G = G(t) = \frac{k_G(\rho\bar{t})}{\rho}$$

$$\text{and} \quad f(x) = \frac{1}{c_k}\bar{f}\left(\sqrt{\frac{\rho}{D_w}}\bar{x}\right)$$

with $N_0 = \int \overline{f}(\overline{x})d\overline{x}$ to denote the initial number of tumor cells in the brain, the model equation in (1) becomes

$$\frac{\partial c}{\partial t} = \nabla\cdot(D\nabla c) + c(1-c) - Rc - Gc\ . \tag{7}$$

We remark that the parabolic nature of the above equation implies continuity of c as well as of both $\partial c/\partial t$ and $D\nabla c$. Therefore, in view of the jump discontinuities of the diffusion, radiotherapy and chemotherapy parameters, described in relations (2), (3) and (6) respectively, appropriate compatibility conditions have to be imposed on the interface between white Ω_w and gray Ω_g matter regions, as well as a proper time schedule has to be followed in order to distinguish and properly implement time intervals with no or any kind of therapy protocol, especially if it is to follow a time step other than the time step of one day.

To be more precise and in order to fix notation let us assume that radiotherapy and chemotherapy are respectively administered in the time intervals

$$T_1 < t \le T_3 \text{ and } T_2 < t \le T_4$$

with

$$0 = T_0 < T_1 < T_2 \le T_3 < T_4 < T_5 = T.$$

Then, the dimensionless IBVP in 1+1 dimensions takes the form:

$$\begin{cases} \dfrac{\partial c}{\partial t} = \dfrac{\partial}{\partial x}\left(D\dfrac{\partial c}{\partial x}\right) + \rho_\ell c - c^2\ ,\ x\in[a,b],\ T_{\ell-1} < t \le T_\ell \\ \dfrac{\partial c}{\partial x}(a,t) = \dfrac{\partial c}{\partial x}(b,t) = 0 \\ c(x,0) = c_\ell(x) \end{cases} \tag{8}$$

where

$$\rho_\ell = \rho_\ell(t) = \begin{cases} 1 & , \quad T_0 < t \le T_1 \\ 1-R & , \quad T_1 < t \le T_2 \\ 1-R-G & , \quad T_2 < t \le T_3 \\ 1-G & , \quad T_3 < t \le T_4 \\ 1 & , \quad T_4 < t \le T_5 \end{cases} \tag{9}$$

and

$$c_\ell(x) = \begin{cases} f(x) & , \quad T_0 < t \le T_1 \\ c(x,T_1) & , \quad T_1 < t \le T_2 \\ c(x,T_2) & , \quad T_2 < t \le T_3 \\ c(x,T_3) & , \quad T_3 < t \le T_4 \\ c(x,T_4) & , \quad T_4 < t \le T_5 \end{cases}\ . \tag{10}$$

Furthermore, let us also assume that there are K interface points w_k in the region $[a,b]$ that distinguish white from gray matter. To be more specific, assume that

$$a = w_0 < w_1 < \cdots < w_k < \cdots < w_K < w_{K+1} = b,$$

and, without any loss of the generality, define

$$\Omega_g = \bigcup_{k=1}^{\lceil K/2\rceil} \mathcal{W}_{2k-1} \quad \text{and} \quad \Omega_w = \bigcup_{k=1}^{\lfloor K/2\rfloor} \mathcal{W}_{2k} \tag{11}$$

with

$$\mathcal{W}_k = (w_{k-1}, w_k)\ , \quad k = 1,\ldots,K+1\ . \tag{12}$$

Then, the required compatibility conditions across each interface point $w_k\ ,\ k=1,\ldots,K$, take the form:

$$\lim_{x\to w_k^-} c(x,t) = \lim_{x\to w_k^+} c(x,t) \tag{13}$$

and

$$\lim_{x\to w_k^-} D(x)c_x(x,t) = \lim_{x\to w_k^+} D(x)c_x(x,t)\ . \tag{14}$$

Finally, we remark that the diffusion coefficient D in (7), is described by:

$$D = D(x) = \begin{cases} \gamma, & \text{when } x \in \Omega_g \\ 1, & \text{when } x \in \Omega_w \end{cases} , \quad (15)$$

where $\gamma = D_g/D_w$.

B. Derivative Discontinuous Hermite Collocation (DHC)

Let us consider a uniform partition of each one of the $k = 1, \ldots, K+1$ regions $\overline{\mathcal{W}}_k = [w_{k-1}, w_k]$ into N_k subintervals of length

$$h_k := \frac{w_k - w_{k-1}}{N_k} . \quad (16)$$

Therefore

$$[a, b] = \bigcup_{j=1}^{N+1} I_j , \quad I_j = [x_{j-1}, x_j] \quad (17)$$

with

$$x_j = a + j\, h_j(k) \quad , \quad j = 0, \ldots, N+1 , \quad (18)$$

where

$$N = \sum_{k=1}^{K+1} N_k \quad \text{and} \quad h_j(k) = h_k \text{ when } I_j \subseteq \overline{\mathcal{W}}_k , \quad (19)$$

for $k = 1, \ldots, K+1$.

The DHC method (cf. [16], [3]) seeks an approximate solutions $u(x,t) \sim c(x,t)$ in the form

$$u(x,t) = \sum_{j=0}^{N+1} [\alpha_{2j}(t)\phi_{2j}(x) + \alpha_{2j+1}(t)\phi_{2j+1}(x)] \quad (20)$$

where the *derivative discontinuous Hermite cubic basis functions* $\phi_{2j}(x)$ and $\phi_{2j+1}(x)$, centered at the node x_j, are defined by

$$\phi_{2j}(x) = \begin{cases} \phi\left(\dfrac{x_j - x}{h_j(k)}\right) & , \quad x \in I_j \\ \phi\left(\dfrac{x - x_j}{h_{j+1}(k)}\right) & , \quad x \in I_{j+1} \\ 0 & , \quad \text{otherwise} \end{cases} , \quad (21)$$

and

$$\phi_{2j+1}(x) = \begin{cases} -\dfrac{h_j(k)}{\gamma_j}\psi\left(\dfrac{x_j - x}{h_j(k)}\right) & , \quad x \in I_j \\ \dfrac{h_{j+1}(k)}{\gamma_{j+1}}\psi\left(\dfrac{x - x_j}{h_{j+1}(k)}\right) & , \quad x \in I_{j+1} \\ 0 & , \quad \text{otherwise} \end{cases} . \quad (22)$$

The functions $\phi(s)$ and $\psi(s)$ are the generating Hermite cubics over $[0,1]$, that is, for $s \in [0,1]$,

$$\phi(s) = (1-s)^2(1+2s) \ , \ \psi(s) = s(1-s)^2 \quad (23)$$

and

$$\gamma_j = \begin{cases} \gamma, & \text{when } I_j \subseteq \Omega_g \\ 1, & \text{when } I_j \subseteq \Omega_w \end{cases} . \quad (24)$$

It can, now, readily be verified that

$$u(x_j, t) = a_{2j}(t), \quad (25)$$

$$u_x(x_j, t) = \begin{cases} a_{2j+1}(t)/\gamma & , \text{ if } x_j \in \Omega_g \bigwedge x_j \neq w_k \ \ \forall k \\ a_{2j+1}(t) & , \text{ if } x_j \in \Omega_w \bigwedge x_j \neq w_k \ \ \forall k \end{cases} , \quad (26)$$

while, whenever $x_j = w_k$, for some k, there holds

$$\lim_{x \to w_k^-} \gamma_j u_x(x,t) = \lim_{x \to w_k^+} \gamma_{j+1} u_x(x,t) \quad (27)$$

hence, the compatibility condition (14) is satisfied.

For the evaluation of the unknown parameters $\alpha_i \equiv \alpha_i(t)$, $i = 0, \ldots, 2(N+1)$ the Collocation method produces a system of ordinary differential equations (ODEs) by forcing the approximate solution $u(x,t)$ to vanish at $2N+2$ *interior collocation* points and the 2 *boundary collocation* points. Collocation at the Gauss points (cf. [8]) adopts the two roots of the Legendre polynomial of degree 2 in each element I_j , $j = 1, \ldots, N+1$ to produce the needed interior collocation points. Namely, the interior Gaussian collocation points for each element I_j are given by

$$\sigma_{2j-1} = \frac{x_{j-1} + x_j}{2} - \frac{h_j}{2\sqrt{3}} \text{ and } \sigma_{2i} = \frac{x_{j-1} + x_j}{2} + \frac{h_j}{2\sqrt{3}}. \quad (28)$$

Substituting, now, $u(x,t)$ of (20) into the equation of the IBVP in (8), observing that in each I_j is an element of four degrees of freedom and noticing that in the interior of each I_j there are no interface points, the two *elemental* collocation equations are written as

$$\begin{aligned} \sum_{L=2j-2}^{2j+1} \dot{\alpha}_L(t)\phi_L(\sigma_i) &= \gamma_j \sum_{L=2j-2}^{2j+1} \alpha_L(t)\phi_L''(\sigma_i) \\ &+ \rho_\ell \sum_{L=2j-2}^{2j+1} \alpha_L(t)\phi_L(\sigma_i) \\ &- \left(\sum_{L=2j-2}^{2j+1} \alpha_L(t)\phi_L(\sigma_i)\right)^2 \end{aligned} \quad (29)$$

for $i = 2j-1$, $2j$ and where, of course, $\dot{\alpha}_L(t) = \dfrac{d}{dt}\alpha_L(t)$ and $\phi_L'(x) = \dfrac{d}{dx}\phi_L(x)$.

Working as in [6], the above elemental equations (29) are expressed in matrix form by:

$$\sum_{L=2j-2}^{2j+1} \alpha_L(t)\phi_L^{(m)}(\sigma_i) = C_j^{(m)}\boldsymbol{\alpha}_j \ , \ i = 2j-1, 2j \ , \quad (30)$$

where

$$C_j^{(m)} = \begin{bmatrix} A_j^{(m)} & B_j^{(m)} \end{bmatrix} , \quad m = 0, 2 \quad (31)$$

$$\boldsymbol{\alpha}_j = \begin{bmatrix} \alpha_{2j-2}(t) & \alpha_{2j-1}(t) & \alpha_{2j}(t) & \alpha_{2j+1}(t) \end{bmatrix}^{\mathrm{T}} \quad (32)$$

ISBN: 978-1-61804-323-8

with

$$A_j^{(m)} = \begin{bmatrix} \phi_{2j-2}^{(m)}(\sigma_{2j-1}) & \phi_{2j-1}^{(m)}(\sigma_{2j-1}) \\ \phi_{2j-2}^{(m)}(\sigma_{2j}) & \phi_{2j-1}^{(m)}(\sigma_{2j}) \end{bmatrix} = \frac{1}{h_j^m} \begin{bmatrix} s_1^{(m)} & \frac{h_j(k)}{\gamma_j} s_2^{(m)} \\ s_3^{(m)} & -\frac{h_j(k)}{\gamma_j} s_4^{(m)} \end{bmatrix}, \quad m = 0, 2 \tag{33}$$

$$B_j^{(m)} = \begin{bmatrix} \phi_{2j}^{(m)}(\sigma_{2j-1}) & \phi_{2j+1}^{(m)}(\sigma_{2j-1}) \\ \phi_{2j}^{(m)}(\sigma_{2j}) & \phi_{2j+1}^{(m)}(\sigma_{2j}) \end{bmatrix} = \frac{1}{h_j^m} \begin{bmatrix} s_3^{(m)} & \frac{h_j(k)}{\gamma_j} s_4^{(m)} \\ s_1^{(m)} & -\frac{h_j(k)}{\gamma_j} s_2^{(m)} \end{bmatrix}, \quad m = 0, 2 \tag{34}$$

and

	$m=0$	$m=2$
$s_1^{(m)}$	$\frac{9+4\sqrt{3}}{18}$	$-2\sqrt{3}$
$s_2^{(m)}$	$\frac{3+\sqrt{3}}{36}$	$-1-\sqrt{3}$
$s_3^{(m)}$	$\frac{9-4\sqrt{3}}{18}$	$2\sqrt{3}$
$s_4^{(m)}$	$-\frac{3-\sqrt{3}}{36}$	$-1+\sqrt{3}$

.

Using, now, the symbol $\circ$ to denote the Hadamard matrix product, the matrix form of the elemental equations in (29) may be written as (see also [6]):

$$\begin{aligned} C_j^{(0)}\dot{\boldsymbol{\alpha}}_j &= \gamma_j C_j^{(2)}\boldsymbol{\alpha}_j + \rho_\ell C_j^{(0)}\boldsymbol{\alpha}_j \\ &- \left(C_j^{(0)}\boldsymbol{\alpha}_j\right) \circ \left(C_j^{(0)}\boldsymbol{\alpha}_j\right) \end{aligned} \tag{35}$$

Moreover, observe that combination of the relations in (26) and the Neumann boundary conditions in (8) immediately implies

$$\alpha_1(t) = \alpha_{2N+3}(t) = 0 \quad , \tag{36}$$

hence, also,

$$\dot{\alpha}_1(t) = \dot{\alpha}_{2N+3}(t) = 0 \quad . \tag{37}$$

The above elemental and boundary collocation equations lead to the non-linear Collocation system of ODEs, described by:

$$C_0\dot{\boldsymbol{\alpha}} = \boldsymbol{\gamma} C_2\boldsymbol{\alpha} + \rho_\ell C_0\boldsymbol{\alpha} - (C_0\boldsymbol{\alpha} \circ C_0\boldsymbol{\alpha}) \tag{38}$$

where the $(2N+2)\times(2N+2)$ matrices $C_m,\ m=0,2$ and $\boldsymbol{\gamma}$ are defined by:

$$C_m = \begin{bmatrix} \tilde{A}_1^{(m)} & B_1^{(m)} & & & & \\ & A_2^{(m)} & B_2^{(m)} & & & \\ & & \ddots & \ddots & & \\ & & & A_N^{(m)} & B_N^{(m)} & \\ & & & & A_{N+1}^{(m)} & \tilde{B}_{N+1}^{(m)} \end{bmatrix}$$

and

$$\boldsymbol{\gamma} = \mathrm{diag}\left(\gamma_1\ \gamma_2\ \gamma_2\ \cdots\ \gamma_N\ \gamma_N\ \gamma_{N+1}\right),$$

while the $2N+2$ vectors $\boldsymbol{\alpha} \equiv \boldsymbol{\alpha}(t)$ and $\dot{\boldsymbol{\alpha}} \equiv \dot{\boldsymbol{\alpha}}(t)$ are described by

$$\boldsymbol{\alpha} = \begin{bmatrix} \alpha_0(t) & \alpha_2(t) & \cdots & \alpha_{2N+1}(t) & \alpha_{2N+2}(t) \end{bmatrix}^{\mathrm{T}}$$

$$\dot{\boldsymbol{\alpha}} = \begin{bmatrix} \dot{\alpha}_0(t) & \dot{\alpha}_2(t) & \cdots & \dot{\alpha}_{2N+1}(t) & \dot{\alpha}_{2N+2}(t) \end{bmatrix}^{\mathrm{T}}.$$

The vectors $\tilde{A}_1^{(k)}$ and $\tilde{B}_{N+1}^{(k)}$ denote the first columns of the matrices $A_1^{(k)}$ and $B_{N+1}^{(k)}$ respectively, as their second columns have been omitted due to the zero boundary conditions.

Concluding this section we point out that the linear independence of the derivative discontinuous Hermite cubic basic functions yields the non-singularity of the matrix C_0 of the Collocation ODE system in (38) implying the existence, of course, of the inverse C_0^{-1}.

C. Implicit-Explicit Runge-Kutta schemes

Implicit-Explicit (IMEX) Runge-Kuttta schemes (cf. [18], [2], [12] and the references therein) are based on implementing an implicit scheme for the stiff part and an explicit scheme for the non or mildly stiff part of a spatial discretized system of ODEs. Here, based on the effective coupling of the Hermite Collocation method with Runge-Kutta schemes we've reported in [3] and [4], we implement an IMEX Runge-Kutta scheme (cf. [17]) that operates on the Collocation system of ODEs in (38) and applies Diagonally Implicit Runge-Kutta (DIRK; cf. [1]) for the linear part and Strong Stability Preserving Runge-Kutta (SSPRK; cf. [23], [24]) for non linear part.

To be more specific, let us write the Collocation system of ODEs in (38) at time level $t = t_n = n\Delta t$ as

$$C_0\dot{\boldsymbol{\alpha}}^{(n)} = \boldsymbol{\gamma} C_2\boldsymbol{\alpha}^{(n)} + \rho_\ell C_0\boldsymbol{\alpha}^{(n)} - \left(C_0\boldsymbol{\alpha}^{(n)} \circ C_0\boldsymbol{\alpha}^{(n)}\right) \tag{39}$$

or, equivalently, as

$$\dot{\boldsymbol{\alpha}}^{(n)} = \mathcal{L}\left(\boldsymbol{\alpha}^{(n)}\right) + \mathcal{N}\left(\boldsymbol{\alpha}^{(n)}\right) \tag{40}$$

where

$$\mathcal{L}\left(\boldsymbol{\alpha}^{(n)}\right) = \boldsymbol{\gamma} C_0^{-1} C_2\boldsymbol{\alpha}^{(n)} + \rho_\ell\boldsymbol{\alpha}^{(n)} \tag{41}$$

and

$$\mathcal{N}\left(\boldsymbol{\alpha}^{(n)}\right) = -C_0^{-1}\left(C_0\boldsymbol{\alpha}^{(n)} \circ C_0\boldsymbol{\alpha}^{(n)}\right) \tag{42}$$

with

$$\dot{\boldsymbol{\alpha}}^{(n)} = \left[\dot{\alpha}_0^{(n)}\ \ \dot{\alpha}_2^{(n)} \cdots \dot{\alpha}_{2N+2}^{(n)}\right]^{\mathrm{T}}$$

and

$$\boldsymbol{\alpha}^{(n)} = \left[\alpha_0^{(n)}\ \ \alpha_2^{(n)} \cdots \alpha_{2N+2}^{(n)}\right]^{\mathrm{T}} \quad .$$

Then, the IMEX Runge-Kutta scheme for the solution of the system in (40) is expressed as (cf. [17]):

$$\begin{aligned} \boldsymbol{\alpha}^{(1)} &= \boldsymbol{\alpha}^{(n)} + \lambda\Delta t\mathcal{L}\left(\boldsymbol{\alpha}^{(1)}\right) \\ \boldsymbol{\alpha}^{(2)} &= \boldsymbol{\alpha}^{(n)} + \Delta t\mathcal{N}\left(\boldsymbol{\alpha}^{(1)}\right) + \Delta t\left(1-2\lambda\right)\mathcal{L}\left(\boldsymbol{\alpha}^{(1)}\right) + \\ &+ \lambda\Delta t\mathcal{L}\left(\boldsymbol{\alpha}^{(2)}\right) \\ \boldsymbol{\alpha}^{(3)} &= \boldsymbol{\alpha}^{(n)} + \frac{\Delta t}{4}\left(\mathcal{N}\left(\boldsymbol{\alpha}^{(1)}\right) + \mathcal{N}\left(\boldsymbol{\alpha}^{(2)}\right)\right) + \end{aligned}$$

$$
\begin{aligned}
&+ \quad \frac{\Delta t(1-2\lambda)}{2}\mathcal{L}\left(\boldsymbol{\alpha}^{(1)}\right) + \lambda\Delta t\mathcal{L}\left(\boldsymbol{\alpha}^{(3)}\right)\\
\boldsymbol{\alpha}^{(n+1)} &= \boldsymbol{\alpha}^{(n)} + \Delta t\left[\mathcal{N}\left(\boldsymbol{\alpha}^{(1)}\right) + \mathcal{N}\left(\boldsymbol{\alpha}^{(2)}\right) + \right.\\
&+ \quad 4\mathcal{N}\left(\boldsymbol{\alpha}^{(3)}\right) + \mathcal{L}\left(\boldsymbol{\alpha}^{(1)}\right) + \mathcal{L}\left(\boldsymbol{\alpha}^{(2)}\right) +\\
&+ \quad \left. 4\mathcal{L}\left(\boldsymbol{\alpha}^{(3)}\right)\right]
\end{aligned}
$$

Finally, we remark that the convergence and stability properties of the above scheme have been studied in [17].

III. Numerical Simulations

In this section, we report the results from the numerical investigation of the performance of the IMEX-DHC method on two virtual model problems.

For both model problems the values of the radiotherapy and chemotherapy parameters used are given by (cf. [20]) $G = 0.0571$ day^{-1} and $R = 0.0196$ day^{-1}, respectively. The radiotherapy protocol followed included equal doses of 1.8Gy per day for 35 days, from day 170 to day 205, while the chemotherapy protocol, starting from day 205, included six cycles of daily treatment for 5 consecutive days followed by a 20 day recess.

A. Model Problem I

For the first single source model, centered at $\bar{x} = 1$, we consider the values:

$$
\begin{cases}
\bar{a} = -10 \text{ cm},\ \bar{b} = 10 \text{ cm},\ \bar{w}_1 = -6 \text{ cm},\ \bar{w}_2 = 8 \text{ cm}\\
\bar{\Omega}_g = [\bar{a}, \bar{w}_1) \cup (\bar{w}_2, \bar{b}] \text{ and } \bar{\Omega}_w = [\bar{w}_1, \bar{w}_2]\\
D_g = 0.0013 \text{ cm}^2\text{day}^{-1},\ D_w = 0.0065 \text{ cm}^2\text{day}^{-1}\\
\bar{\rho} = 0.012 \text{ day}^{-1}\ ,\ N_0 = 2 \times 10^4 \text{ cells}
\end{cases}.
$$

The results form the numerical simulation are depicted in Figs. 1 and 2, as well as in Table I.

More specifically, Fig. 1 depicts the evolution of the cell density function $\bar{c}(\bar{x}, \bar{t})$. One may easily identify periods of untreated and treated tumor growth.

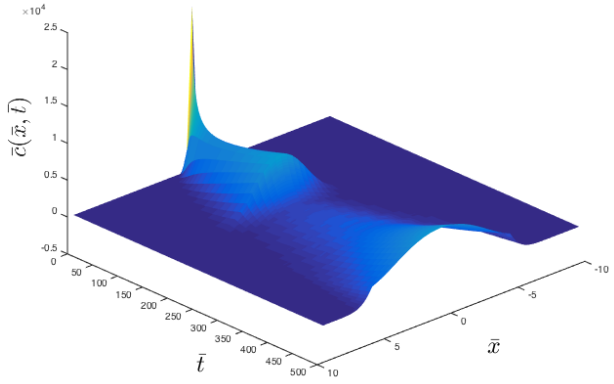

Fig. 1: Time evolution of the cell density $\bar{c}(\bar{x}, \bar{t})$

The radiotherapy effect on the total number of tumor cells $\bar{N}(\bar{t})/N_0$, where $N(\bar{t}) = \int_{\bar{a}}^{\bar{b}} \bar{c}(\bar{x}, \bar{t})d\bar{x}$, is depicted in Fig. 2.

Finally, Table I summarizes the performance of the DHC-IMEX method. One may easily observe the 4-th order of convergence of the DHC method.

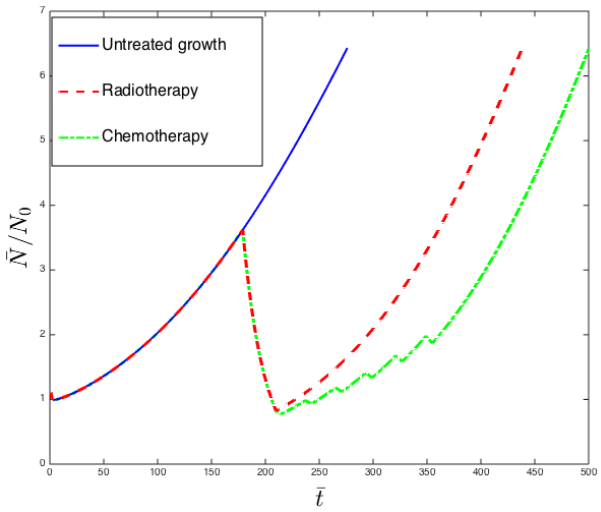

Fig. 2: The effect of radiotherapy on the total number of tumor cells.

Table I DCH-IMEX Performance

h	Error	O.o.c.	Time (sec)
1/8	3.5687e-06	-	0.24
1/16	2.3357e-07	3.93	0.30
1/32	1.4760e-08	3.98	0.42
1/64	9.2474e-10	3.99	0.88
1/128	5.6156e-11	4.04	1.55

B. Model Problem II

For the triple source model we consider the values:

$$
\begin{cases}
\bar{a} = -10 \text{ cm},\ \bar{b} = 10 \text{ cm},\ \bar{w}_1 = -4 \text{ cm},\ \bar{w}_2 = 6 \text{ cm}\\
\bar{\Omega}_g = [\bar{a}, \bar{w}_1) \cup (\bar{w}_2, \bar{b}] \text{ and } \bar{\Omega}_w = [\bar{w}_1, \bar{w}_2]\\
D_g = 0.0013 \text{ cm}^2\text{day}^{-1},\ D_w = 0.0065 \text{ cm}^2\text{day}^{-1}\\
\bar{\rho} = 0.012 \text{ day}^{-1}\ ,\ N_0 = 2 \times 10^4 \text{ cells}
\end{cases}
$$

All results are summarized in Figs. 3 and 4 as well as Table II and are completely similar to the corresponding ones of the previous model case.

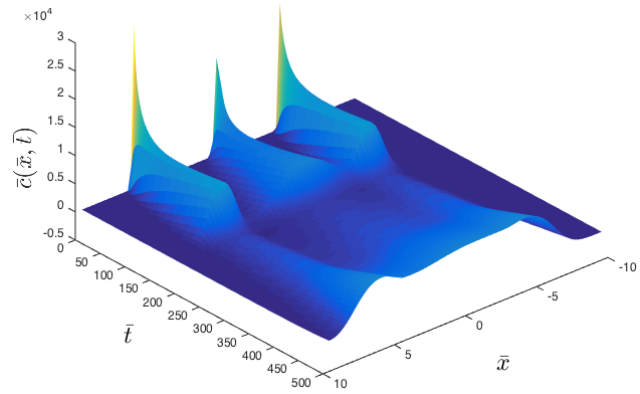

Fig. 3: Time evolution of the cell density $\bar{c}(\bar{x}, \bar{t})$.

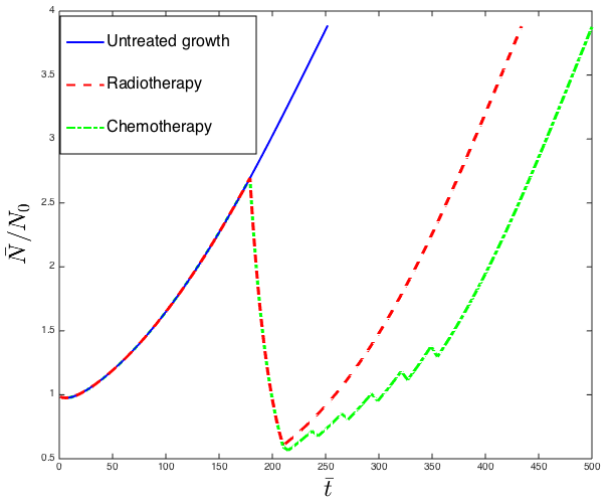

Fig. 4: The effect of radiotherapy and chemotherapy on the total number of tumor cells.

Table II DCH-IMEX Performance

h	Error	O.o.c.	Time (sec)
1/8	5.3380e-06	-	0.22
1/16	3.4585e-07	3.94	0.28
1/32	2.1802e-08	3.98	0.40
1/64	1.3655e-09	3.99	0.90
1/128	8.5010e-11	4.00	1.52

IV. Conclusion

We have developed and investigated the performance of a high order Derivative Discontinuous Hermite Collocation, coupled with an IMEX Runge-Kutta scheme, for the solution of a quasi-linear reaction diffusion IBVP that models the brain tumor growth taking into consideration brain's heterogeneity and the effects of radiotherapy and chemotherapy. The results obtained justify and encourage further analysis as well as implementation in higher dimensions.

Acknowledgment

The present research work has been co-financed by the European Union (European Social Fund ESF) and Greek national funds through the Operational Program Education and Lifelong Learning of the National Strategic Reference Framework (NSRF) - Research Funding Program: THALES (Grant number: MIS-379416). Investing in knowledge society through the European Social Fund.

References

[1] R. Alexander, *Diagonally Implicit Runge-Kutta Methods for stiff ODE's*, SIAM Num. Anal., vol. 14, no. 6, pp. 1006-1021, 1977.

[2] U. M. Ascher, S. J. Ruuth and R. J. Spiteri, *Implicit-Explicit Runge-Kutta Methods for Time-Dependent Partial Differential Equations*, Applied Numerical Mathematics, 25, 151-167, 1997

[3] I. E. Athanasakis, M. G. Papadomanolaki, E. P. Papadopoulou and Y. G. Saridakis, *Discontinuous Hermite Collocation and Diagonally Implicit RK3 for a Brain Tumor Invasion Model*, Procs WCE-ICAEM, 1, 241-246, 2013.

[4] I. E. Athanasakis, E. P. Papadopoulou and Y. G. Saridakis, *Runge-Kutta and Hermite Collocation for a biological invasion problem modeled by a generalized Fisher equation*, Journal of Physics: Conference Series, 490, 012133, 2014.

[5] I.E. Athanasakis, E.P. Papadopoulou and Y.G. Saridakis, *Discontinuous Tensor Product Collocation and Runge-Kutta schemes for heterogeneous brain tumor invasion models*, (in Preparation) 2015.

[6] I.E. Athanasakis, E.P. Papadopoulou and Y.G. Saridakis, *Hermite Collocation and SSPRK Schemes for the Numerical Treatment of a Generalized Kolmogorov-Petrovskii-Piskunov Equation*, Procs WCE-ICAEM 2015.

[7] S. M. Blinkov and I. Glezer, *The Human Brain in Figures and Tables*, New York: Plenum Press, 1968.

[8] C. de Boor and B. Swartz, *Collocation at Gaussian points*, SIAM Num. Anal., vol.10, pp. 582-606, 1973.

[9] P.K. Burgess, P.M. Kulesa, J.D. Murray and E.C. Alvord Jr, *The interaction of growth rates and diffusion coefficients in a three-dimensional mathematical model of gliomas*, Journal of Neuropathology and Experimental Neurology, vol.56, no. 6, pp.704-713, 1997.

[10] D. Corwin, C. Holdsworth, R. C. Rockne, An. D. Trister, M. M. Mrugala, J. K. Rockhill, R. D. Stewart2, M. Phillips2 and K. R. Swanson, *Toward Patient-Specific, Biologically Optimized Radiation Therapy Plans for the Treatment of Glioblastoma*, PLOS ONE, 8(11), 1-9, 2013

[11] G.C. Cruywagen, D.E. Woodward, P. Tracqui, G.T. Bartoo, J.D. Murray and E.C. Alvord Jr, *The modeling of diffusive tumors*, Journal of Biological Systems , vol.3, pp.937-945, 1995.

[12] T. Koto, *IMEX RungeKutta schemes for reactiondiffusion equations*, J Comp. App. Math., 215, 182 195, 2008

[13] J.D. Murray, *Mathematical Biology I and II*, Springer-Verlag, 3rd Edition 2002.

[14] P. Nilsson, H. D. Thames and M. C. Joiner, *A generalized formulation of the incomplete-repair model for cell survival and tissue response to fractionated low dose-rate irradiation*, Int. J. Radiat. Biol., 57, 12742, 1990.

[15] M.G. Papadomanolaki, *The collocation method for parabolic differential equations with discontinuous diffusion coefficient: in the direction of brain tumor simulations*, PhD Thesis, Technical University of Crete, 2012 (in Greek)

[16] M.G. Papadomanolaki and Y.G. Saridakis, *Hermite-Collocation for one dimensional tumor invasion model with heterogeneous diffusion*, HERMIS-$\mu\pi$, vol. 11, pp.63-68, 2010.

[17] L. Pareschi and G. Russo, *ImplicitExplicit RungeKutta Schemes and Applications to Hyperbolic Systems with Relaxation*, J. Scient. Comp., 25(1), 129-155, 2005

[18] S. J. Ruuth, *Implicit-Explicit Methods For Reaction-Diffusion Problems In Pattern Formation*, J. Math. Biology, 34, 148-176, 1995

[19] K.R.Swanson, *Mathematical modelling of the growth and control of tumor*, PHD Thesis, University of Washington, 1999.

[20] G. Powathil, M. Kohandel, S. Sivaloganathan, A. Oza2 and M Milosevic, *Mathematical modeling of brain tumors: effects of radiotherapy and chemotherapy*, Phy. Med. Biol. 52, 3291-3306, 2007.

[21] R. Rockne, E. C. Alvord Jr., J. K. Rockhill and K. R. Swanson, *A mathematical model for brain tumor response to radiation therapy*, J. Math. Biol., 58, 561578, 2009.

[22] R. D. Russel and L.F. Shampine, *A collocation method for boundary value problems* Numer. Math. , 19(1) pp. 128, 1972.

[23] C. W. Shu, *Total-variation-diminishing time discretizations*, SIAM J. Sci. Stat. Comput., **9**, 1073-1084, 1988

[24] C. W. Shu and S. Osher, *Efficient implementation of essentially non-oscillatory shock-capturing schemes*, J. Comput. Phys., **77**, 439-471, 1988

[25] K.R.Swanson, E.C.Alvord Jr and J.D.Murray, *A quantitive model for differential motility of gliomas in grey and white matter*, Cell Proliferation, vol.33, pp.317-329, 2000.

[26] K. R. Swanson,C. Bridge, J. D. Murray and E. C. Alvord Jr, *Virtual and real brain tumors:using mathematical modeling to quantify glioma growth and invasion*, J.Neurol.Sci, vol.216, pp.1-10, 2003.

[27] P.Tracqui,G.C.CruywagenG,D.E.Woodward,T.Bartoo, J.D.Murray and E.C.Alvord Jr, *A mathematical model of glioma growth:The effect of chemotherapy on spatio-temporal growth*, *Cell Proliferation*, vol.28, pp.17-31, 1995.

[28] D.E.Woodward,J.Cook,P.Tracqui,G.C.Cruywagen,J.D.Murray,and E.C.Alvord Jr, *A mathematical model of glioma growth: the effect of extent of surgical resection*, *Cell Proliferation*, vol.29, pp.269-288, 1996.